Sea level observations using multi-system GNSS reflectometry

Johan S. Löfgren & Rüdiger Haas
Chalmers University of Technology, Department of Earth and Space Sciences,
Onsala Space Observatory, SE-439 92 Onsala (Sweden)
e-mail: johan.lofgren@chalmers.se, rudiger.haas@chalmers.se

Introduction

Information on sea level and its changes are important in connection to global climate change processes. For centuries, sea level has been observed with coastal tide gauges and since some decades with satellite altimetry. Furthermore, during recent years the application of Global Navigation Satellite System (GNSS) reflectometry, also known as GNSS-R, for sea level observations has been developed, see e.g., Martin-Neira M. (1993), Lowe *et al.* (2002), Gleason *et al.* (2005), Löfgren *et al.* (2011a,b; 2014), Larson *et al.* (2013a,b), and Löfgren & Haas (2014). Various methods exist, using ground-based, airborne and space-borne systems, and using different analysis methods. We present results from a dedicated GNSS tide gauge installed at the Onsala Space Observatory at the Swedish west coast. This installation consists of commercially-off-the-shelf GNSS equipment, including geodetic-type choke-ring antennas and geodetic-type receivers and allows for analysis using both phase and Signal-to-Noise Ratio (SNR) data.

The GNSS tide gauge installation

The GNSS tide gauge consists of two antennas mounted on a beam extending in southward direction over the coastline. The antennas are aligned along the local vertical, with one antenna facing toward zenith direction and the other facing toward nadir, see **Fig. 1**. The zenith-looking antenna is Right-Hand-Circular-Polarised (RHCP) while the nadir-looking antenna is Left-Hand-Circular-Polarised (LHCP). The zenith-looking antenna receives predominantly the direct RHCP satellite signals, while the nadir-looking antenna receives predominantly signals that are reflected off the sea surface and thus have changed polarization to LHCP in the reflection process.

Each antenna (Leica AR25 multi-GNSS choke-ring) is connected to a GNSS receiver of model Leica GRX1200 GG PRO. Each receiver individually record multi-frequency signals of several GNSS with 1 Hz sampling rate. The signals used for this study are Global Positioning System (GPS) and GLObalnaya NAvigatsionnaya Sputnikovaya Sistema (GLONASS) carrier-phase and Signal-to-Noise Ratio (SNR) data (recorded with resolution 0.25 dBHz) in both L-band frequency bands. More information about the installation is given in Löfgren & Haas (2014) and Löfgren *et al.* (2014).

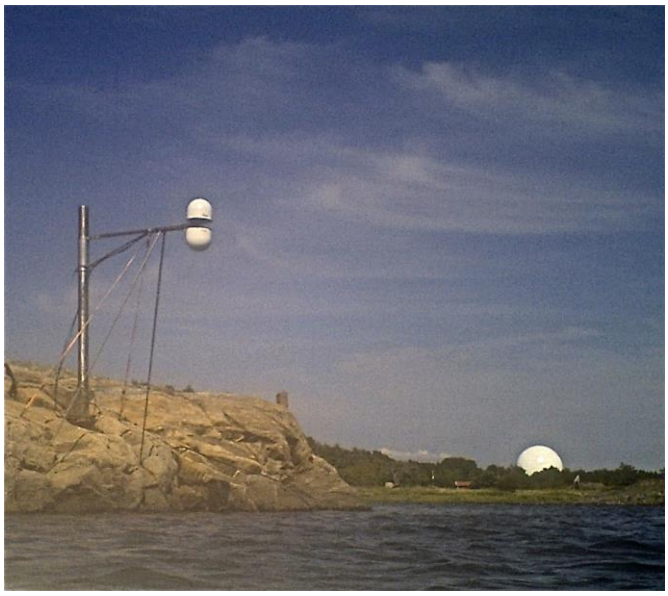

Fig. 1. *The GNSS tide gauge installation, with one zenith-looking and one nadir-looking antenna (covered by hemispherical radomes), at the Onsala Space Observatory in Sweden. The radome of the 20 metre radio telescope is visible in the background.*

Analysis methods

The recorded GNSS data can be analysed in two different ways to derive information on the sea level and its variation. In the first analysis strategy, carrier-phase data are used from both the zenith-looking RHCP antenna and the nadir-looking LHCP antenna. As previously described, the zenith-looking antenna receives the direct RHCP satellite signals, working in the same way as a geodetic GNSS station and the nadir-looking antenna receives the satellite signals that have reflected off the sea surface. Depending on the elevation angle of the transmitting satellite, the signal will change polarization after reflection. After reflection off the sea surface, most of the signal will turn into a LHCP signal (LHCP is dominant for reflections from elevation angles of about 10 to 90 degrees) and is thus received by the receiver connected to the nadir-looking LHCP antenna.

With this in mind, data from both receivers can be analysed together applying geodetic-type phase-delay analysis with, e.g., a single-difference or double-difference strategy, see Löfgren *et al.* (2011a,b), Löfgren (2014), and Löfgren & Haas (2014). These analysis methods determine the baseline between the two antennas (or actually the baseline between the zenith-looking antenna and the nadir-looking antenna mirrored in the sea surface), which is proportional to the height of the installation above the sea surface. This distance will change with a changing sea surface.

In the second analysis strategy, SNR data are used from only the zenith-looking RHCP antenna. The single zenith-looking installation is the standard setup for any geodetic GNSS station and the SNR-strategy can therefore be used for any GNSS installation close to the ocean, see Larson *et al.* (2013a,b), Löfgren (2014) and Löfgren *et al.* (2014).

Even though the RHCP antenna is designed to receive GNSS signals from the upper hemisphere and suppress signals from the lower hemisphere, i.e., signals reflected in the surroundings, a portion of the satellite signals that have reflected off the sea surface will reach the antenna. These reflected signals (also called multipath signals) interfere with the direct satellite signals and the composite signals are recorded by the GNSS receiver. This effect is most dominant for signals from lower satellite elevations (about 0 to 30 degrees) and depends on the antenna gain pattern in combination with the reflected signal polarisation, which is dominantly RCHP for low satellite elevations (about 0 to 10 degrees) and then decreasing for increasing satellite elevation.

This interference effect is especially visible in the recorded SNR of the zenith-looking antenna and the multipath oscillations in the SNR can be used to derive the distance between the sea surface and the antenna. Again, this distance will change with a changing sea surface.

The two different analysis strategies have advantages and disadvantages. Furthermore, the sea level results from both strategies can be combined with standard positioning of the zenith-looking antenna to give absolute sea level information, i.e. sea level with respect to the International Terrestrial Reference Frame.

Sea level results

The GNSS-derived sea level was compared to independent sea level observations from a co-located traditional tide gauge (pressure sensors). As an example, sea level time series from both analysis strategies, phase-analysis and SNR-analysis, both systems, GPS and GLONASS, and both frequency bands, L_1 and L_2, are presented in **Fig. 2** for 20 days in 2012 (October 9 to 29). In addition, a combined phase-analysis solution of GPS and GLONASS data is shown

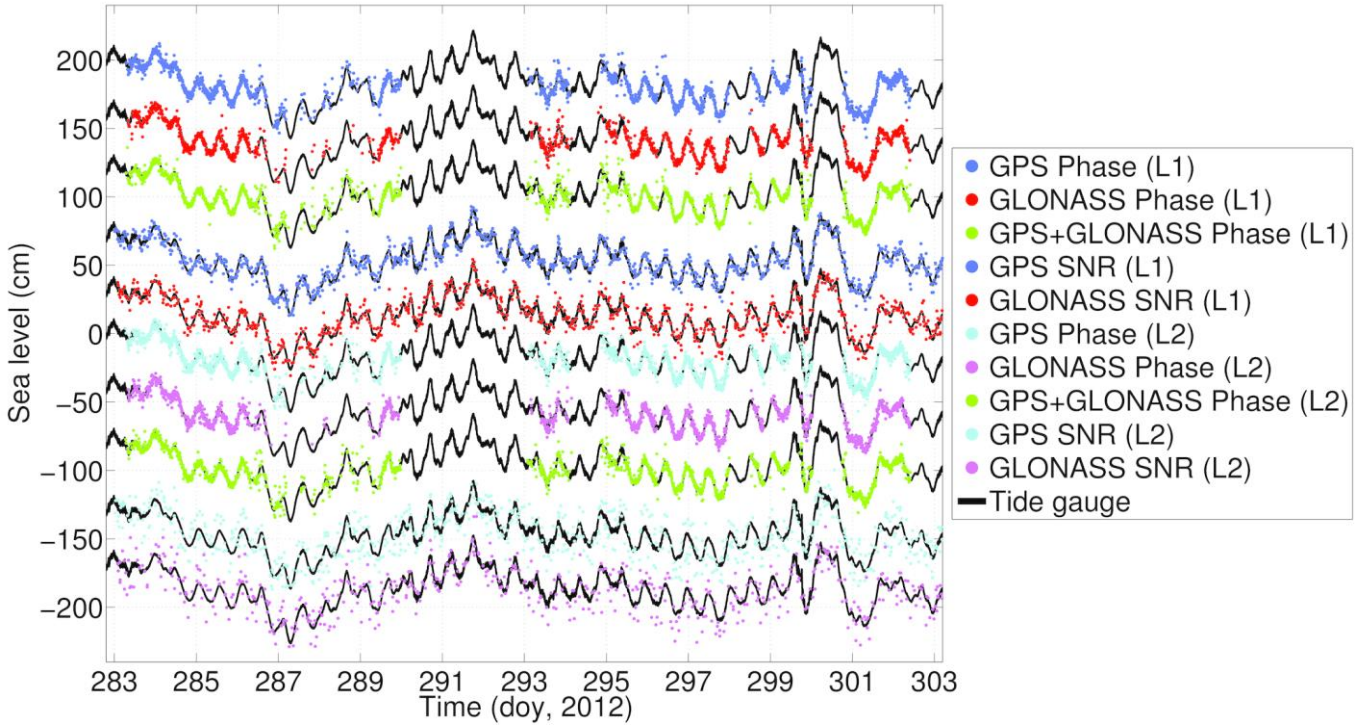

Fig. 2. *Sea level derived from the GNSS tide gauge at the Onsala Space Observatory during 20 days in 2012 (October 9 to 29). From top to bottom the sea level times series are derived from: GPS phase (L_1), GLONASS phase (L_1), GPS and GLONASS phase (L_1), GPS SNR (L_1), GLONASS SNR (L_1), GPS phase (L_2), GLONASS phase (L_2), GPS and GLONASS phase (L_2), GPS SNR (L_2) and GLONASS SNR (L_2). Each time series is paired with the independent sea level observations from the co-located tide gauge (black line). A mean is removed from each time series and the pairs are displayed with an offset of 40 cm to improve visibility.*

Tab. 1. *Comparison of GNSS-derived sea level, for both the SNR-analysis strategy and the phase-analysis strategy, and the sea level from the co-located traditional tide gauge. Shown are results from GPS-only, GLONASS-only, and from multiple-GNSS analysis (GPS+GLONASS).*

		GPS		GLONASS		GPS+GLONASS	
		L1	**L2**	**L1**	**L2**	**L1**	**L2**
SNR	**Solutions (nr)**	1516	1229	1254	882		
	Correlation coefficient	0.97	0.86	0.96	0.87		
	Standard deviation (cm)	4.0	8.9	4.7	8.9		
Phase	**Solutions (nr)**	1534	1495	1408	1286	1581	1484
	Correlation coefficient	0.95	0.95	0.96	0.96	0.95	0.96
	Standard deviation (cm)	3.5	3.5	3.3	3.2	3.7	3.4

for both L_1 and L_2 in **Fig. 2**. The times series are compared in a relative sense, i.e., a mean is removed for each time series. In **Fig. 2**, each GNSS time series is displayed together with the time series from the co-located traditional tide gauge and each time series pair is offset from each other by 40 cm to increase visibility.

From **Fig. 2**, it is possible to conclude that all GNSS-derived time series show the same sea level variations as seen by the co-located traditional tide gauge. The time series resulting from the SNR-analysis are noisier than those resulting from the phase-analysis and the sea level from SNR-analysis of the data from frequency band L_2 (not GPS L_{2C}) appears to be the noisiest. Furthermore, there are gaps in the phase analysis time series, which are not present in the SNR analysis time series. This is consistent with previous studies, see Löfgren *et al.* (2011b) and Löfgren & Haas (2014), showing that the geodetic GNSS receiver has problems tracking the reflected signal in rough sea surface conditions. However, the SNR solutions (with data from the zenith-looking antenna) appear to be unaffected by the sea surface roughness in this study.

In order to quantify the comparison between the GNSS-derived sea level and the sea level observations from the co-located traditional tide gauge, the correlation coefficient and the standard deviation are calculated for each time series pair seen in **Fig. 2**. The results of the comparison are presented in **Tab. 1**.

First of all, the high correlation coefficients of 0.86 to 0.97, shown in **Tab. 1**, demonstrate the strong agreement between the traditional tide gauge sea level observations and the GNSS-derived sea level. The correlation coefficients for the phase-analysis strategy, for separate and combined GPS and GLONASS analysis, show similar results for both frequency bands (0.95 to 0.96). However, for the SNR-analysis strategy, the results from frequency band L_1 shows a better agreement to the tide gauge sea level than the results from frequency band L_2, with correlation coefficients of 0.96 to 0.97 and 0.86 to 0.87, respectively.

The values of the standard deviation for the phase-analysis are on the same order (3.2 to 3.7 cm) for both systems (separate and combined) and for both frequency bands, see **Tab. 1**. This is better than for the SNR-analysis, where the standard deviation is lower for frequency band L_1 than for frequency band L_2 with values of 4.0 to 4.7 and 8.9, respectively.

There are no combined solutions for the SNR-analysis, see **Tab. 1**. The reason is that each observed satellite arc is analysed separately (compare with the phase-analysis where all observations are combined in a least-squares solution each epoch). However, one option for "combination" of the SNR-analysis results would be to merge the GPS and GLONASS time series into a single GNSS SNR time series.

A comment should also be made regarding the number of solutions for the respective analysis strategies in **Tab. 1**, which appear to be more or less the same for the 20 days. This is because of the previously explained problems for the geodetic receiver connected to the nadir-looking antenna with tracking the reflected signals in rough sea surface conditions. The actual rate of solutions or temporal resolution for the SNR-analysis is about 30 to 50 solutions per day and for the phase-analysis the same number is 144 continuous solutions per day for this study. Furthermore, the temporal resolution of the phase-analysis solutions can be as high as the sampling rate of the GNSS receiver.

Conclusion

The aim of this study was to show sea level results obtained from GNSS reflectometry data from the GNSS tide gauge at the Onsala Space Observatory and compare them to sea level observations from a co-located traditional tide gauge. Two analysis strategies have been presented: SNR-analysis, using SNR data from one zenith-looking RHCP antenna (can be used with data from any GNSS station close to the ocean), and phase-analysis, using phase data from both a zenith-looking RHCP antenna and a nadir-looking LHCP antenna together. The two strategies have been applied to multi-

system data (GPS and GLONASS data) in both the L_1 and L_2 frequency band. In addition to separate analysis for the data of the two systems, GPS and GLONASS data have been combined for the phase-analysis.

In comparison between the GNSS-derived sea level and sea level from the co-located traditional tide gauge, the correlation coefficients were 0.86 to 0.97, showing that the variations in the sea level are well represented by the GNSS observations.

Our results show that the phase-analysis strategy with GPS and GLONASS, using signals in the L_1 and L_2 frequency bands, gives a standard deviation on the order of 3-4 cm when compared to the independently observed sea level observations from the co-located traditional tide gauge. The corresponding results derived from the SNR-analysis strategy are worse by a factor of about 1.5 and 3 for the L_1 and L_2 (not L_{2C}) frequency bands, respectively. However, the SNR-analysis method appears to have advantages in conditions of high sea surface roughness. Furthermore, no major differences can be seen in the results from GPS and GLONASS data, i.e. both systems appear to provide equally good sea level observations.

As previously mentioned, the standard deviation values of the combined solution are on the same level as that of the separate solutions (perhaps even slightly higher than expected). The phase-analysis combination was done without consideration of inter-system biases (GNSS and receiver dependent) and antenna phase centre corrections. A future multi-system solution could therefore benefit from the inclusion of parameters for these biases and corrections.

Future plans for the the two analysis strategies are to, in addition to GPS and GLONASS observations, include multi-frequency observations from Galileo and BeiDou and to evaluate the sea level results against sea level from other GNSS reflectometry techniques and new traditional tide gauges at the Onsala Space Observatory.

As suggested, merging the SNR-analysis sea level results from the different systems can be beneficial by, e.g., increasing the temporal resolution of the sea level time series. Another future improvement could be to use both analysis strategies in a filter approach in order to benefit from the individual advantages.

References

Gleason S., Hodgart S., Sun Y., Gommenginger C., Mackin S., Adjrad M.,Unwin M. (2005): Detection and Processing of bistatically reflected GPS signals from low Earth orbit for the purpose of ocean remote sensing. *Trans. Geosci. Remote Sensing* 43(6), 1229-1241.

Larson K.M., Löfgren J.S., Haas R. (2013a): Coastal sea level measurements using a single geodetic GPS receiver. *Adv. Space Res* 51(8), 1301-1310.

Larson K.M., Ray R.D., Nievinski F.G., Freymueller J.T. (2013b): The accidental tide gauge: a case study of GPS reflections from Kachemak Bay, Alaska. *IEEE GRSL* 10(5), 1200-1205.

Lowe S.T., Zuffada C., Chao Y., Kroger P., Young L.E., LaBrecque J.L. (2002): 5-cm-Precision aircraft ocean altimetry using GPS reflections. *Geophys. Res. Lett.* 29(10), 4 p.

Löfgren J.S., Haas R., Johansson J.M. (2011a): Monitoring coastal sea level using reflected GNSS signals. *J. Adv. Space Res.* 47(2), 213-220.

Löfgren J.S., Haas R., Scherneck H.-G., Bos M.S. (2011b): Three months of local sea level derived from reflected GNSS signals. *Radio Sci.* 46, 12 p.

Löfgren J.S. (2014): Local sea level observations using reflected GNSS signals. *PhD dissertation*, Department of Earth and Space Sciences, Chalmers University of Technology, 62 p.

Löfgren J.S., Haas R. (2014): Sea level measurements using multi-frequency GPS and GLONASS observations. *EURASIP J. Adv. Sig. Pr.* 2014:50, 13 p.

Löfgren J.S., Haas R., Scherneck H.-G. (2014): Sea level time series and ocean tide analysis from multipath signals at five GPS sites in different parts of the world. *J. Geodyn.* 80, 66-80.

Martin-Neira M. (1993): A PAssive Reflectometry and Interferometry System (PARIS): Application to ocean altimetry. *ESA J.* 17, 331–355.